PHYSICAL REVIEW A **00**, 003800 (2011)

Multidimensional phase-sensitive single-molecule spectroscopy with time-and-frequency-gated fluorescence detection

Shaul Mukamel[1,*] and Marten Richter[1,2]

[1]*Department of Chemistry, University of California, Irvine, California 92697-2025, USA*

[2]*Institut für Theoretische Physik, Nichtlineare Optik und Quantenelektronik, Technische Universität Berlin, Hardenbergstrasse 36, 10623 Berlin, Germany*

(Received 22 September 2010; published xxxxx)

$(n+1)$-dimensional gated fluorescence signals induced by n impulsive pulses are calculated using a superoperator formalism. The signals are given by a time-and-frequency convolution of a bare signal, expressed in terms of multipoint dipole correlation functions, with a gating spectrogram. Different groups of quantum pathways can be separated by their variation with the phases of the pulses (phase cycling), as is commonly done in nuclear magnetic resonance. Comparison is made with heterodyne-detected coherent signals.

DOI: 10.1103/PhysRevA.00.003800 PACS number(s): 42.50.Ct, 42.62.Fi, 82.53.Kp, 87.80.Nj

I. INTRODUCTION

Coherent multidimensional signals are usually detected by interference with a reference (local oscillator) beam [1–3]. This heterodyne-detection mode provides both the amplitude and the phase of the signal field. Various groups of Liouville space pathways of the molecular density matrix that contribute to the signal may be separated by simply looking at signals generated in different phase-matching directions. A different, incoherent fluorescence detection is, however, the method of choice for single-molecule spectroscopy, since it is more sensitive and background-free [4–6]. Fluorescence is virtually isotropic in space; nevertheless, the groups of pathways may be separated by their dependence on the phases of the pulses. This phase-cycling protocol is common in nuclear magnetic resonance [7–10], where the signal is isotropic as well, since the sample is much smaller than the wavelength.

Coherent wave-mixing spectroscopies detect a macroscopic electric field generated by a collection of molecules driven in phase by the external laser pulses. Fluorescence is an incoherent technique: it does not generate a macroscopic field (the average field vanishes), but produces photons that can be detected. Fluorescence signals do not carry phase information but this can be retrieved by time-and-frequency gating [2,11–15].

Both coherent and incoherent signals can be recorded vs several parameters of the incoming pulses, thus producing multidimensional signals. Fluorescence induced by multiple phase-controlled pulses and no gating have been carried out in bulk samples by several groups [16–21]. The technique was recently extended to single molecules [22]. Single-molecule spectroscopy typically resolves slow fluctuation timescales (milliseconds and longer) [4,23]. Gated fluorescence signals offer a powerful femtosecond window for ultrafast molecule events, thus combining high spatial and temporal resolution.

In this paper, we use an intuitive diagrammatic representation for incoherent signals to derive closed microscopic correlation function expressions for multidimensional spectroscopy with gated fluorescence detection. The driving laser pulses are treated as classical, but a quantum description of the detected optical field is used. An application is made to a three-band exciton model system. Bulk signals can be calculated by a slight modification of the single-molecule results.

II. INCOHERENT SIGNALS GENERATED IN RESPONSE TO SEQUENCES OF IMPULSIVE PULSES

Our description of incoherent signals starts with the light-matter Hamiltonian in the rotating-wave approximation [24,25]:

$$H = H_0 + H', \tag{1}$$

$$H' = -E^\dagger(\boldsymbol{r}=0,t)V - E(\boldsymbol{r}=0,t)V^\dagger, \tag{2}$$

where the field operator $E^\dagger(\boldsymbol{r},t) + E(\boldsymbol{r},t)$ and the dipole operator $V^\dagger + V$ have been partitioned into their negative and positive frequency parts. The molecule is located at position $\boldsymbol{r}=0$. To describe the fluorescence signal, $E(\boldsymbol{r},t)$ is taken as a field operator for the spontaneous emitted modes and a classical function for the other modes, which represent the incoming laser pulses.

We shall calculate the fluorescence detected using a gate, whose input is located at $\boldsymbol{r}_G$, which consists of a time gate F_t centered at time t_0 followed by a frequency gate F_s centered at frequency ω_0 [2,12–14]. The temporal gate first transforms the signal field as

$$E_t(\boldsymbol{r}_G,t') = F_t(t',t_0)E(\boldsymbol{r}_G,t'). \tag{3}$$

By applying the spectral gate centered at ω_0, we obtain the time-and-frequency-gated field $E_{ts}(\omega') = F_s(\omega';\omega_0)E_t(\omega')$, with $E(\omega) = \int_{-\infty}^{\infty} E(t)e^{i\omega t}dt$. Note that the signal depends on the order of gating operations. Applying the spectral gate first will result in a different signal that can be calculated similarly, as shown in Appendix C. Combining the two gates, the gated field E_{ts} is finally related to the original (bare) signal field by

$$E_{ts}(\boldsymbol{r}_D,t) = \int_{-\infty}^{\infty} dt_1 F_s(t-t_1,\omega_0)F_t(t_1,t_0)E(\boldsymbol{r}_G,t_1), \tag{4}$$

where $\boldsymbol{r}_D$ is the position of the photon detector. To simplify the notation the propagation between $\boldsymbol{r}_G$ and $\boldsymbol{r}_D$ is included inside the spectral gate function.

*smukamel@uci.edu

The gated fluorescence signal is given by [11,26,27]

$$S(\omega_0,t_0;\Gamma)=\int_{-\infty}^{\infty}dt''\langle E_{ts}^{\dagger}(\boldsymbol{r}_D,t'')E_{ts}(\boldsymbol{r}_D,t'')\rangle, \tag{5}$$

where the angular brackets in the correlation function are defined as $\langle\cdots\rangle=\mathrm{tr}(\cdots\rho)$. Here Γ denotes a set of parameters that characterizes the incoming laser pulses. These will be specified later. The signal will be displayed vs these parameters as well as the gating parameters ω_0 and t_0. We further define the *bare signal* (which is not generally an experimental observable)

$$S_B(t_1,\omega';\Gamma)=\int_0^{\infty}d\tau\langle E^{\dagger}(\boldsymbol{r}_D,t_1+\tau)E(\boldsymbol{r}_D,t_1)\rangle e^{-i\omega'\tau}d\tau. \tag{6}$$

We shall also introduce the gating spectrogram [12,14]:

$$\begin{aligned}&W(\omega_0,t_0;\omega',t_1)\\&\quad=\frac{1}{2\pi}\int_{-\infty}^{\infty}dt''\int_{-\infty}^{\infty}d\tau e^{i\omega'\tau}F_s^*(t''-t_1-\tau,\omega_0)\\&\qquad\times F_t^*(t_1+\tau;t_0)F_s(t''-t_1;\omega_0)F_t(t_1;t_0).\end{aligned} \tag{7}$$

It can be also recast in the form

$$W(\omega_0,t_0;\omega',t_1)=\int_{-\infty}^{\infty}\frac{d\omega}{(2\pi)^2}|F_s(\omega,\omega_0)|^2W_t(t_1,\omega-\omega',t_0), \tag{8}$$

where

$$W_t(t_1,\omega;t_0)=\int_{-\infty}^{\infty}F_t^*(t_1,t_0)F_t(t_1+\tau,t_0)\,e^{i\omega\tau}d\tau. \tag{9}$$

By combining Eqs. (4)–(9) we get the final expression for the signal:

$$\begin{aligned}&S(\omega_0,t_0;\Gamma)\\&\quad=\int_{-\infty}^{\infty}dt_1\int_{-\infty}^{\infty}d\omega'W(\omega_0,t_0;\omega',t_1)S_B(t_1,\omega';\Gamma)+\text{c.c.}\end{aligned} \tag{10}$$

The gating spectrogram thus connects the observed S and the bare S_B signals and controls the temporal and spectral resolution of the measurement.

To connect the bare signal S_B with the molecular properties, we use the solution of the wave equation with a point-dipole source V located at the origin $\boldsymbol{r}=0$ (see Appendix B) [28]:

$$E(\boldsymbol{r}_G,t)=A\ddot{V}_H(0,t-|\boldsymbol{r}_G|/c). \tag{11}$$

The prefactor A is given by Eq. (B6). To simplify the expressions, we will omit in the following the time retardation, assuming that the time scale at the detector is adjusted accordingly [t_1 on the left-hand side of Eq. (12), and following should read $t_1+|\boldsymbol{r}_G|/c$]. Substituting Eq. (11) in Eq. (6), we obtain for the bare signal

$$S_B(t_1,\omega';\Gamma)=|A|^2\int_0^{\infty}d\tau e^{-i\omega'\tau}\langle\ddot{V}_H^{\dagger}(t_1+\tau)\ddot{V}_H(t_1)\rangle. \tag{12}$$

The subscript H indicates that these operators are in the Heisenberg picture, that is, that they evolve with the full Hamiltonian, Eq. (2).

We shall adopt a superoperator notation, which allows to derive compact expressions in Liouville space and clearly reveals the relevant pathways [1,29–31]. For any operator A we define the "left" and "right" superoperators $A_LX=AX$, $A_RX=XA$ by their action on any other operator X. We further introduce the two linear combinations $A_+=\frac{1}{2}(A_L+A_R)$, $A_-=A_L-A_R$. These definitions imply that $A_+X=\frac{1}{2}(AX+XA)$ and $A_-X=AX-XA$. Using the superoperator representation of the interaction picture [30,31], we get

$$\begin{aligned}&S_B(t_1,\omega';\Gamma)\\&\quad=|A|^2\int_0^{\infty}d\tau e^{-i\omega'\tau}\partial_{t_1+\tau}^2\partial_{t_1}^2\mathrm{tr}\Big[TV_R^{\dagger}(t_1+\tau)V_L(t_1)\\&\qquad\times\exp\Big(-\frac{i}{\hbar}\int_0^{\infty}d\tau_1H'_-(\tau_1)\Big)\rho_0\Big].\end{aligned} \tag{13}$$

The operators V are in the interaction picture defined as

$$V(t)=\exp(iH_0t/\hbar)V\exp(-iH_0t/\hbar), \tag{14}$$

and here we used the formal expression for the density matrix:

$$\rho(t)=T\exp\left(-\frac{i}{\hbar}\int_0^t H'_-(\tau)\,d\tau\right)\rho_0. \tag{15}$$

Here T is the time-ordering operator, which rearranges the super operators to its right in order of increasing time from right to left. We are using partial derivatives, since the entire expression inside the trace can be viewed as a function of the variables $t_1+\tau$ and t_1 [cf. Eq. (12)].

Equation (13) is the key formal result of this paper. Together with Eq. (10) we have thus recasted the gated signal in terms of the underlying microscopic molecular dynamics.

We next consider two limiting cases for the detection. For an ideal frequency gating, when no time gating is applied, we can set $F_t(t',t_0)=1$ and obtain

$$\begin{aligned}&W(\omega_0,t_0;\omega',t_1)\\&\quad=\frac{1}{2\pi}\int_{-\infty}^{\infty}dt''\int_{-\infty}^{\infty}d\tau e^{i\omega'\tau}\\&\qquad\times F_s^*(t''-t_1-\tau,\omega_0)F_s(t''-t_1;\omega_0).\end{aligned} \tag{16}$$

Assuming $F_s(\tau;\omega_0)=e^{-i\omega_0\tau}e^{-\gamma\tau}\theta(\tau)$ with $\gamma\to\infty$, we obtain the ideal spectral gate:

$$W(\omega_0,t;\omega',t_1)=\delta(\omega'-\omega_0). \tag{17}$$

Substituting Eq. (17) in Eq. (10) gives the spectral resolved signal:

$$S_s(\omega_0;\Gamma)=\int_{-\infty}^{\infty}dt_1S_B(t_1,\omega_0;\Gamma)+\text{c.c.} \tag{18}$$

Combining with Eq. (12), we finally obtain

$$\begin{aligned}&S_s(\omega_0;\Gamma)\\&\quad=|A|^2\int_{-\infty}^{\infty}dt_1\int_0^{\infty}d\tau e^{-i\omega_0\tau}\partial_{t_1+\tau}^2\partial_{t_1}^2\mathrm{tr}\Big[TV_R^{\dagger}(t_1+\tau)\\&\qquad\times V_L(t_1)\exp\Big(-\frac{i}{\hbar}\int_0^{\infty}d\tau_1H'_-(\tau_1)\Big)\rho_0\Big]+\text{c.c.}\end{aligned} \tag{19}$$

Assuming that the density matrix at time t_1 is diagonal, that the coherent pulses and the gate are well separated, and that

there are no photons in the system at t_1, we get the following for the matter density matrix ρ_e:

$$\rho_e(t_1) = \sum_n P_n(t_1)|n\rangle\langle n|, \tag{20}$$

$$P_n(t_1) = \mathrm{tr}\left[|n\rangle\langle n|T\exp\left(-\frac{i}{\hbar}\int_0^{t_1} d\tau_1 H'_-(\tau_1)\right)\rho_0\right], \tag{21}$$

if the molecule can be described by a nuch of levels n. Equation (19) then becomes

$$S_s(\omega_0;\Gamma) = B\sum_{m<n}\omega_{nm}\Gamma_{nm}\int_{-\infty}^{\infty} dt_1 P_n(t_1)\delta(\omega_0-\omega_{nm}), \tag{22}$$

where the sum runs over molecule states with $\varepsilon_m < \varepsilon_n$ and $B = 3\pi^2|A|^2c^3\varepsilon_0/\hbar$, with $\omega_{nm} = \varepsilon_m - \varepsilon_n$. $\Gamma_{mn} = \frac{\omega_{nm}^3|V_{nm}|^2\hbar}{3\pi c^3\varepsilon_0}$ is the radiative decay rate from state m to n [24].

The signal in this limit can be alternatively derived by summing over the temporal derivative of the photon number n_i of all modes with frequency ω_0 and integrating over time:

$$S_s(\omega_0;\Gamma) \propto \sum_{i,\omega_i=\omega_0}\int_{-\infty}^{\infty}\partial_t n_i(t)\,dt. \tag{23}$$

We next turn to the second limiting case of ideal temporal gating. Here, we assume no frequency gating and set $F_s(\tau,\omega_0) = \delta(\tau)$:

$$W(\omega_0,t_0;\omega',t_1) = \frac{1}{2\pi}F_t^*(t_1;t_0)F_t(t_1;t_0). \tag{24}$$

Taking a short time filter with $|F_t(t_1,t_0)|^2 = \delta(t_1-t_0)$ we get the ideal temporal gate:

$$W(\omega_0,t_0;\omega',t_1) = \frac{1}{2\pi}\delta(t_1-t_0). \tag{25}$$

Substitution of this in Eq. (12) gives the temporally resolved signal:

$$S_t(\omega_0,t;\Gamma) = \frac{1}{2\pi}\int_{-\infty}^{\infty} d\omega' S_B(t,\omega';\Gamma) + \text{c.c.} \tag{26}$$

Inserting Eq. (13) gives

$$\begin{aligned} &S_t(\omega_0,t;\Gamma)\\ &= \frac{|A|^2}{2\pi}\int_{-\infty}^{\infty}d\omega'\int_0^{\infty}d\tau e^{-i\omega'\tau}\partial_{t+\tau}^2\partial_t^2\mathrm{tr}\Big[TV_R^\dagger(t+\tau)\\ &\quad\times V_L(t)\exp\left(-\frac{i}{\hbar}\int_0^{\infty}d\tau_1 H'_-(\tau_1)\right)\rho_0\Big] + \text{c.c.} \end{aligned} \tag{27}$$

The integrations can now be carried out and this finally gives

$$\begin{aligned} S_t(t;\Gamma) &= |A|^2\partial_{t+\tau}^2\partial_t^2\mathrm{tr}\Big[TV_R^\dagger(t)V_L(t+\tau)\\ &\quad\times\exp\left(-\frac{i}{\hbar}\int_0^{\infty}d\tau_1 H'_-(\tau_1)\right)\rho_0\Big]\Big|_{\tau=0} + \text{c.c.} \end{aligned} \tag{28}$$

In order to simplify this formula further, we again assume that the matter density matrix is given by Eqs. (20) and (21) and the signal finally becomes

$$S_t(t;\Gamma) = \sum_n B\Gamma_n P_n(t), \tag{29}$$

$$\Gamma_n = \sum_{m<n}\omega_{nm}\Gamma_{nm}. \tag{30}$$

The spectrum in this limit can be alternatively derived by summing over the temporal derivative of the photon number n_i of all modes with frequency ω_0:

$$S(t;\Gamma) \propto \sum_{i,\omega_i}\omega_i\partial_t n_i(t). \tag{31}$$

III. FLUORESCENCE OF A THREE-BAND MODEL SYSTEM IN RESPONSE TO FOUR IMPULSIVE PULSES

We now apply the formal expressions derived earlier to the three-band model system shown in Fig. 1 subjected to four temporally well-separated excitation pulses:

$$\begin{aligned} E(t) = {}& E_1(t)e^{i\omega_1 t+i\varphi_1} + E_2(t-t_1)\,e^{i\omega_2 t+i\varphi_2}\\ &+ E_3(t-t_1-t_2)e^{i\omega_3 t+i\varphi_3}\\ &+ E_4(t-t_1-t_2-t_3)\,e^{i\omega_4 t+i\varphi_4} + \text{c.c.} \end{aligned} \tag{32}$$

The pulse envelopes $E_j(t)$ are temporally well separated, and we assume impulsive fields $E_i(t) = E_i\delta(t)$. Furthermore, hereafter we treat the four excitation pulses as classical. This generic model can represent, for example, excitons in molecular aggregates or semiconductors.

The density matrix Eq. (15) calculated to the fourth order in the fields has $2^4 = 16$ pathways:

$$\rho^{(4)} = \left(\frac{-i}{\hbar}\right)^4 H'_-G(t_3)H'_-G(t_2)H'_-G(t_1)H'_-\rho_0, \tag{33}$$

with the interaction picture operators $H'_-(t) = \exp(\frac{i}{\hbar}H_0t)H'_-\exp(-\frac{i}{\hbar}H_0t)$ and $G(t) = \theta(t)\exp(-\frac{i}{\hbar}H_0-t)$. $\theta(t)$ is the Heaviside step function that ensures causality.

When recast in Hilbert space, Eq. (33) reads

$$\begin{aligned} \rho^{(4)} = {}& \left(\frac{-i}{\hbar}\right)^4[H'(t_1+t_2+t_3),\\ &[H'(t_1+t_2),[H'(t_1),[H',\rho_0]]]]. \end{aligned} \tag{34}$$

Equation (34) can be divided into 16 groups of terms with respective phases $\pm\varphi_1\pm\varphi_2\pm\varphi_3\pm\varphi_4$. Each of these groups can be measured using phase-cycling protocol, which

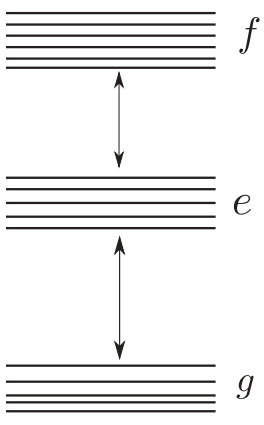

FIG. 1. The three-band model system used to calculate the fluorescence signal.

combines experiments with different phases [7–10] (Fig. 2). Hereafter we select the phase $\phi = \varphi_1 + \varphi_2 - \varphi_3 - \varphi_4$; signals with other phases can be calculated similarly. Within the rotating- wave approximation, the density matrix corresponding to the phase shown in Fig. 3 has four contributions labeled (i)–(iv):

$$\rho_{\phi}^{(4)}(t_1+t_2+t_3) = \left(\sum_{g_1 g_2} \rho_i(g_1,g_2)|g_1\rangle\langle g_2| + \sum_{e_2 e_3} \rho_{ii}(e_2,e_3)|e_2\rangle\langle e_3| + \sum_{e_2 e_3} \rho_{iii}(e_2,e_3)|e_2\rangle\langle e_3| + \sum_{f_1 f_2} \rho_{iv}(f_1,f_2)|f_1\rangle\langle f_2| \right). \quad (35)$$

To simplify the expressions we assume impulsive pulse $E_i(t) = E_i\delta(t)$. We then get

$$\rho_{\rm i}(g_1,g_2) = \left(\frac{-i}{\hbar}\right)^4 {\rm tr}[|g_2\rangle\langle g_1|V_L G(t_3)V_L G(t_2)V_L^{\dagger} G(t_1)V_L^{\dagger}\rho_0]E_{\phi}, \quad (36)$$

$$\rho_{\rm ii}(e_2,e_3) = -\left(\frac{-i}{\hbar}\right)^4 {\rm tr}[|e_3\rangle\langle e_2|V_R G(t_3)V_L G(t_2)V_L^{\dagger} G(t_1)V_L^{\dagger}\rho_0]E_{\phi}, \quad (37)$$

$$\rho_{\rm iii}(e_2,e_3) = -\left(\frac{-i}{\hbar}\right)^4 {\rm tr}[|e_3\rangle\langle e_2|V_R G_{fl_3}(t_3)V_L G(t_2)V_L^{\dagger} G(t_1)V_L^{\dagger}\rho_0]E_{\phi}, \quad (38)$$

$$\rho_{\rm iv}(f_1,f_2) = \left(\frac{-i}{\hbar}\right)^4 {\rm tr}[|f_2\rangle\langle f_1|V_R G(t_3)V_R G(t_2)V_L^{\dagger} G(t_1)V_L^{\dagger}\rho_0]E_{\phi}, \quad (39)$$

where we have defined the auxiliary parameter:

$$E_{\phi} = e^{i\varphi_1 + i\varphi_2 - i\varphi_3 - i\varphi_4} E_1 E_2 E_3^* E_4^* e^{i(\omega_2-\omega_3-\omega_4)t_1 - i(\omega_3+\omega_4)t_2 - i\omega_4 t_3}. \quad (40)$$

Equations (36)–(39) can be transformed to Hilbert space:

$$\rho_{\rm i}(g_1,g_2) = \left(\frac{-i}{\hbar}\right)^4 \langle g_1|V(t_1+t_2+t_3)V(t_1+t_2)V^{\dagger}(t_1)V^{\dagger}(0)\rho_0|g_2\rangle E_{\phi}, \quad (41)$$

$$\rho_{\rm ii}(e_2,e_3) = -\left(\frac{-i}{\hbar}\right)^4 \langle e_2|V(t_1+t_2)V^{\dagger}(t_1)V^{\dagger}(0)\rho_0 V(t_1+t_2+t_3)|e_3\rangle E_{\phi}, \quad (42)$$

$$\rho_{\rm iii}(e_2,e_3) = -\left(\frac{-i}{\hbar}\right)^4 \langle e_2|V(t_1+t_2+t_3)V^{\dagger}(t_1)V^{\dagger}(0)\rho_0 V(t_1+t_2)|e_3\rangle E_{\phi}, \quad (43)$$

$$\rho_{\rm iv}(f_1,f_2) = \left(\frac{-i}{\hbar}\right)^4 \langle f_1|V^{\dagger}(t_1)V^{\dagger}(0)\rho_0 V(t_1+t_2)V(t_1+t_2+t_3)|f_2\rangle E_{\phi}. \quad (44)$$

We now expand Eqs. (36)–(39) in eigenstates and use the approach of [32] to incorporate the finite pulse envelopes:

$$\rho_{\rm i}(g_1,g_2) = \frac{1}{\hbar^4}\sum_{e_1,e_2,f} P_{0,g_1}V_{g_2e_2}V_{e_2f}V_{fe_1}V_{e_1g_1}E_1(\omega_{e_1g_1}-\omega_1)E_2(\omega_{fe_1}-\omega_2)E_3^*(\omega_{fe_2}-\omega_3)E_4^*(\omega_{e_2g_2}-\omega_4)$$
$$\times \exp\left(-i\omega_{e_2g_1}t_3 - \gamma_{e_2g_1}t_3 - i\omega_{fg_1}t_2 - \gamma_{fg_1}t_2 - i\omega_{e_1g_1}t_1 - \gamma_{e_1g_1}t_1\right), \quad (45)$$

$$\rho_{\rm ii}(e_2,e_3) = -\frac{1}{\hbar^4}\sum_{g_1,e_1,f} P_{0,g_1}V_{e_2f}V_{fe_1}V_{e_1g_1}V_{g_1e_3}E_1(\omega_{e_1g_1}-\omega_1)E_2(\omega_{fe_1}-\omega_2)E_3^*(\omega_{fe_2}-\omega_3)E_4^*(\omega_{e_3g_1}-\omega_4)$$
$$\times \exp\left(-i\omega_{e_2g_1}t_3 - \gamma_{e_2g_1}t_3 - i\omega_{fg_1}t_2 - \gamma_{fg_1}t_2 - i\omega_{e_1g_1}t_1 - \gamma_{e_1g_1}t_1\right), \quad (46)$$

$$\rho_{\rm iii}(e_2,e_3) = -\frac{1}{\hbar^4}\sum_{e_1,f,g_1} P_{0,g_1}V_{e_2f}V_{fe_1}V_{e_1g_1}V_{g_1e_3}E_1(\omega_{e_1g_1}-\omega_1)E_2(\omega_{fe_1}-\omega_2)E_3^*(\omega_{e_3g_1}-\omega_3)E_4^*(\omega_{fe_2}-\omega_4)$$
$$\times \exp\left(-i\omega_{fe_3}t_3 - \gamma_{fe_3}t_3 - i\omega_{fg_1}t_2 - \gamma_{fg_1}t_2 - i\omega_{e_1g_1}t_1 - \gamma_{e_1g_1}t_1\right), \quad (47)$$

$$\rho_{\rm iv}(f_1,f_2) = \frac{1}{\hbar^4}\sum_{e_1,e_2,g_1} P_{0,g_1}V_{f_1e_1}V_{e_1g_1}V_{g_1e_2}V_{e_2f_2}E_1(\omega_{e_1g_1}-\omega_1)E_2(\omega_{f_1e_1}-\omega_2)E_3^*(\omega_{e_2g_1}-\omega_3)E_4^*(\omega_{f_2e_2}-\omega_4)$$
$$\times \exp\left(-i\omega_{f_1e_2}t_3 - \gamma_{f_1e_2}t_3 - i\omega_{f_1g_1}t_2 - \gamma_{f_1g_1}t_2 - i\omega_{e_1g_1}t_1 - \gamma_{e_1g_1}t_1\right). \quad (48)$$

Here, we have defined $P_{0,v} \equiv P_v(t=0)$.

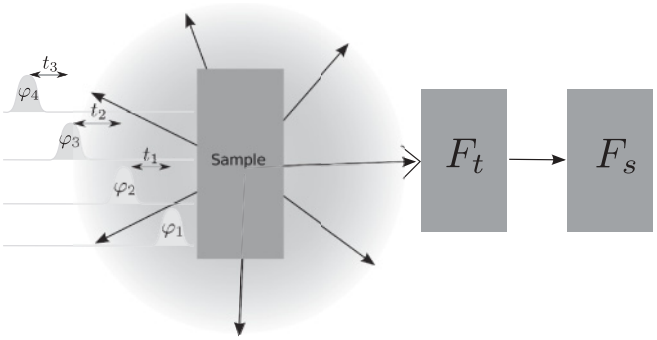

FIG. 2. Experimental setup for the gated fluorescence measurement.

We used for the example of Eqs. (45)–(48) the coherent limit, where the Green function matrix elements in the system eigenstate basis ν read

$$G_{\nu\nu'}(t) = \theta(t)\exp(-i\omega_{\nu\nu'}t - \gamma_{\nu\nu'}t), \tag{49}$$

where $\omega_{\nu\nu'}$ is the frequency and $\gamma_{\nu\nu'}$ is the dephasing rate of the $\nu\nu'$ transition. More complex relaxation models may be used together with the equations before and the following equations [1,33]. For example, G can depend on a set of collective bath coordinates Q that satisfy a Markovian dynamics (master equation, Fokker-Planck equation, etc.). We then have $G(Q,Q',t)$ and the correlation functions are given by path integrals over the trajectories of Q. G can describe how states shift due to solvent reorganization [1].

Assuming fast dephasing, $\rho^{(4)}$ becomes diagonal and we have $\sum_{e_2}\rho_{\rm ii}(e_2,e_2) = -\sum_{g_1}\rho_{\rm i}(g_1,g_1)$ and $\sum_{e_2}\rho_{\rm iii}(e_2,e_2) = -\sum_{f_1}\rho_{\rm iv}(f_1,f_1)$ we then get

$$\rho_D^{(4)} = \left(\sum_{e_2} P_{{\rm ii},e_2}|e_2\rangle\langle e_2| - \sum_{g_1} P_{{\rm i},g_1}|g_1\rangle\langle g_1|\right) + \left(\sum_{f_1} P_{{\rm iv},f_1}|f_1\rangle\langle f_1| + \sum_{e_1} P_{{\rm iii},e_1}|e_1\rangle\langle e_1|\right), \tag{50}$$

$$\begin{aligned} P_{{\rm ii},e_2} &= \rho_{\rm ii}(e_2,e_2), \quad P_{{\rm i},g_1} = \rho_{\rm i}(g_1,g_1), \\ P_{{\rm iii},e_1} &= \rho_{\rm iii}(e_1,e_1), \quad P_{{\rm iv},f_1} = \rho_{\rm iv}(f_1,f_1). \end{aligned} \tag{51}$$

It is clear from Eq. (50) that $\mathrm{tr}(\rho_s^{(4)}) = 0$. This follows immediately from Eq. (33) since this is given by the trace of a commutator. In fact, the trace of all $\rho^{(n)}$, $n = 1,2,\ldots$ must vanish so that the trace of $\rho^{(0)}$ is conserved.

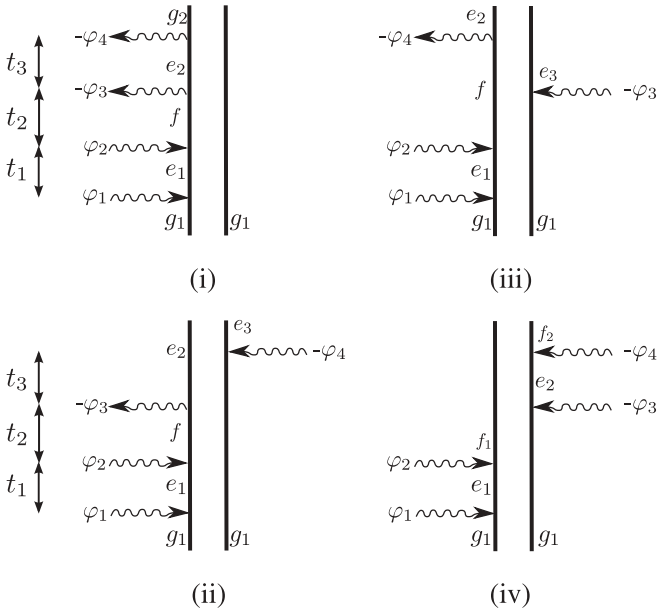

FIG. 3. The density matrix of the system shown in Fig. 1 driven by four impulsive pulses. We have selected the contributions with phase $\phi = \varphi_1 + \varphi_2 - \varphi_3 - \varphi_4$ [Eq. (35)].

If we do not resolve the fluorescence into states, the signal is given by the total excited-state population given by the sum of three terms $\rho_{\rm ii}, \rho_{\rm iii}$, and $\rho_{\rm iv}$. If we distinguish the states—through either their temporal [Eq. (29)] or spectral fluorescence profile [Eq. (22)]—we can separate the P_e and P_f contributions.

Substituting Eq. (33) in Eq. (13), we obtain for the bare time-and-frequency-resolved fluorescence signal

$$\begin{aligned} &S_B(\omega',t',t_3,t_2,t_1) \\ &\quad = \frac{|A|^2}{\hbar^4}\int_0^\infty \left\{\partial_{t'+\tau}^2\partial_{t'}^2\,\mathrm{tr}[V_R^\dagger G(\tau)V_L G(t')H'_- G(t_3) \right. \\ &\qquad \left. \times H'_- G(t_2)H'_- G(t_1)H'_-\rho_0]\right\}\exp(-i\omega'\tau)\,d\tau. \end{aligned} \tag{52}$$

This includes all contributions $\pm\varphi_1 \pm \varphi_2 \pm \varphi_3 \pm \varphi_4$. Substituting in Eq. (10) yields a five-dimensional signal (we now denote $t = t_4$)

$$\begin{aligned} &S(\omega,t_4,t_3,t_2,t_1) \\ &\quad = \mathrm{Re}\int_{-\infty}^\infty dt'\int_{-\infty}^\infty d\omega' S_B(\omega',t',t_3,t_2,t_1)W(\omega,t_4;\omega',t'). \end{aligned} \tag{53}$$

Translating the superoperators into Hilbert space, the bare signal reads

$$\begin{aligned} S_B(\omega',t',t_3,t_2,t_1) = \frac{|A|^2}{\hbar^4}E_\phi\int_0^\infty &\exp(-i\omega'\tau)\partial_{t'+\tau}^2\partial_{t'}^2\,\mathrm{tr}\{V^\dagger(t_1+t_2+t_3+t'+\tau)V(t_1+t_2+t_3+t')[H'(t_1+t_2+t_3), \\ &[H'(t_1+t_2),[H'(t_1),[H'(0),\rho_0]]]]\}d\tau. \end{aligned} \tag{54}$$

We shall now select the contribution with phase $\phi = \varphi_1 + \varphi_2 - \varphi_3 - \varphi_4$ and obtain for the gated fluorescence [Eq. (10)]

$$S_\phi(\omega_0,t;\Gamma) = \int_{-\infty}^\infty dt_1\int_{-\infty}^\infty d\omega' W(\omega_0,t;\omega',t_1)S_\phi^a(t_1,\omega';\Gamma) + \int_{-\infty}^\infty dt_1\int_{-\infty}^\infty d\omega' W^*(\omega_0,t;\omega',t_1)S_\phi^b(t_1,\omega';\Gamma). \tag{55}$$

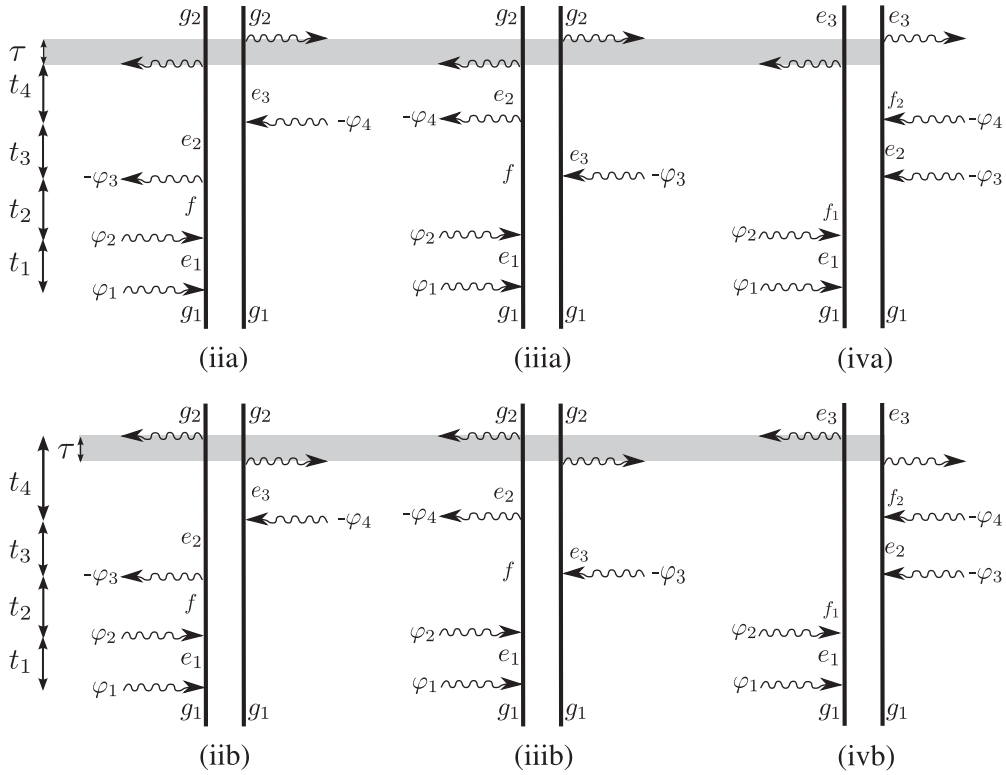

FIG. 4. Multidimensional fluorescence signal of the model system of Fig. 1 induced by four impulsive pulses with phase $\phi = \varphi_1 + \varphi_2 - \varphi_3 - \varphi_4$.

Here the contributions S^a_ϕ and S^b_ϕ represent the bare signal S_B (see diagrams of Fig. 4). We have three contributions to S^a_ϕ [pathways with (a)] and three contributions to S^b_ϕ [pathways with (b)]:

$$S^a_\phi = S_{\rm iia} + S_{\rm iiia} + S_{\rm iva}, \tag{56}$$

$$S^b_\phi = S_{\rm iib} + S_{\rm iiib} + S_{\rm ivb}, \tag{57}$$

$$S_{\rm iia}(\omega',t_4,t_3,t_2,t_1) = \frac{|A|^2}{\hbar^4} E_\phi \int_0^\infty d\tau \exp(-i\omega'\tau)\partial^2_{t_4+\tau}\partial^2_{t_4}\,{\rm tr}[V_R^\dagger G(\tau)V_L G(t_4)V_R G(t_3)V_L G(t_2)V_L^\dagger G(t_1)V_L^\dagger \rho_0], \tag{58}$$

$$S_{\rm iib}(\omega',t_4,t_3,t_2,t_1) = \frac{|A|^2}{\hbar^4} E_\phi \int_0^\infty d\tau \exp(-i\omega'\tau)\partial^2_{t_4+\tau}\partial^2_{t_4}\,{\rm tr}[V_L G(\tau)V_R^\dagger G(t_4)V_R G(t_3)V_L G(t_2)V_L^\dagger G(t_1)V_L^\dagger \rho_0], \tag{59}$$

$$S_{\rm iiia}(\omega',t_4,t_3,t_2,t_1) = \frac{|A|^2}{\hbar^4} E_\phi \int_0^\infty d\tau \exp(-i\omega'\tau)\partial^2_{t_4+\tau}\partial^2_{t_4}{\rm tr}[V_R^\dagger G(\tau)V_L G(t_4)V_L G(t_3)V_R G(t_2)V_L^\dagger G(t_1)V_L^\dagger \rho_0], \tag{60}$$

$$S_{\rm iiib}(\omega',t_4,t_3,t_2,t_1) = \frac{|A|^2}{\hbar^4} E_\phi \int_0^\infty d\tau \exp(-i\omega'\tau)\partial^2_{t_4+\tau}\partial^2_{t_4}\,{\rm tr}[V_L G(\tau)V_R^\dagger G(t_4)V_L G(t_3)V_R G(t_2)V_L^\dagger G(t_1)V_L^\dagger \rho_0], \tag{61}$$

$$S_{\rm iva}(\omega',t_4,t_3,t_2,t_1) = -\frac{|A|^2}{\hbar^4} E_\phi \int_0^\infty d\tau \exp(-i\omega'\tau)\partial^2_{t_4+\tau}\partial^2_{t_4}\,{\rm tr}[V_R^\dagger G(\tau)V_L G(t_4)V_R G(t_3)V_R G(t_2)V_L^\dagger G(t_1)V_L^\dagger \rho_0], \tag{62}$$

$$S_{\rm ivb}(\omega',t_4,t_3,t_2,t_1) = -\frac{|A|^2}{\hbar^4} E_\phi \int_0^\infty d\tau \exp(-i\omega'\tau)\partial^2_{t_4+\tau}\partial^2_{t_4}\,{\rm tr}[V_L G(\tau)V_R^\dagger G(t_4)V_R G(t_3)V_R G(t_2)V_L^\dagger G(t_1)V_L^\dagger \rho_0]. \tag{63}$$

In Appendix D we expand these expressions in the system states. Again we make use of the approach developed in [32], which allows us to include finite pulse envelopes (temporally well separated but not impulsive pulses). The total fluorescence from state e is given by $\rho_{\rm ii}$ and $\rho_{\rm iii}$ and the fluorescence from f is given by $\rho_{\rm iv}$.

The corresponding coherent heterodyne-detected signal generated at $\varphi_4 = \varphi_1 + \varphi_2 - \varphi_3$ is depicted in Fig. 5. For completeness, we derive this signal in Appendix A [Eq. (A8)].

IV. DISCUSSION

Coherent heterodyne-detected signals generated by n fields (including the local oscillator) constitute an $(n-1)D$ phase-sensitive spectroscopy obtained by varying the $n-1$ delay

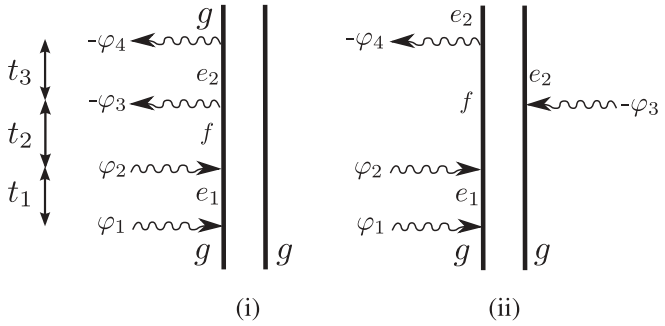

FIG. 5. Coherent signal with phase $\varphi_4 = \varphi_1 + \varphi_2 - \varphi_3$, Eq. (A8).

periods. The total incoherent fluorescence signal induced by n pulses is also $(n-1)D$. Additional (either spectral or temporal) resolution of the final emitting state makes it nD and allows to separate some groups of pathways. Time-and-frequency gating turns the technique into $(n+1)D$. Equations (D1) through (D6) give the fluorescence signal with phase $\phi = \varphi_1 + \varphi_2 - \varphi_3 - \varphi_4$ and $n = 4$.

The superoperator formalism allows the derivation of exact compact formal expressions for all possible signals. Each technique depends on a different combination of pathways. Coherent signals [Eq. (A1)] depend on any number of V_- operators but the last interaction must be V_L (in fact, due to invariance of the trace the last V_L can be replaced by V_R or V_+ without affecting the result). Fluorescence, in contrast, contains several V_- followed by *two* operators corresponding to the detected photons: one V_L and the other V_R. Coherent signals are given by causal response functions. Fluorescence is noncausal since in this technique at least one field mode is correlated with the material system and the signal is a combination of response and spontaneous fluctuations [29,34].

With small modifications the results of this article also apply to signals from bulk samples. The field produced at distance z by a sheet of identical emitting dipoles with η dipoles per unit area is [28]

$$E(\boldsymbol{r},t) = -\frac{\eta}{2\varepsilon_0 c}\dot{V}_H(0,t-z/c). \tag{64}$$

Equation (12) now reads

$$S_B(t_1,\omega';\Gamma) = |A_s|^2 \int_0^\infty d\tau e^{-i\omega'\tau}\langle \dot{V}_H^\dagger(t_1+\tau)\dot{V}_H(t_1)\rangle, \tag{65}$$

with $A_S = -\eta/(2\varepsilon_0 c)$. All our results apply except that the prefactor A is modified and only a first instead of a second time derivative is applied to the last two interactions. In the frequency domain we have for a single-point dipole source,

$$E(\boldsymbol{r},\omega) = -\frac{1}{\varepsilon_0 c^2}\omega^2 \frac{e^{i(\omega/c)|\boldsymbol{r}|}}{4\pi|\boldsymbol{r}|}V(0,\omega), \tag{66}$$

compared with the bulk formula for a sheet:

$$E(\boldsymbol{r},\omega) = -i\omega\frac{1}{2\varepsilon_0 c}e^{i(\omega/c)|z|}\eta V(0,\omega). \tag{67}$$

The extra i factor implies a $\pi/2$ phase shift between the two fields.

In our calculations (Fig. 4), we assumed that the gating is temporally well separated from the excitation pulses. The V_L and V_R operators are therefore the last. We note, however, that Eq. (13) is more general and can also describe Raman processes, where other time ordering contributes. In each diagram either V_L or V_R must be the last but the other one can be at any time; fluorescence is generated by pathways, where the V_L and V_R are temporally well separated from the excitation pulses. Otherwise we have additional Raman pathways.

Finally, we would like to point out the possible extension to a different incoherent technique: time-resolved photoelectron spectroscopy, where electrons rather than photons are detected. Phase-sensitive photoelectron detection has been reported [35–37]. Multidimensional photoelectron spectroscopy can be calculated by combining the present results with the formalism of [38,39]. This will be an interesting topic for future study.

ACKNOWLEDGMENTS

The support of the National Science Foundation (Grant No. CHE-0745892), DARPA BAA-10-40 QuBE and the Chemical Sciences, Geosciences and Biosciences Division, Office of Basic Energy Sciences, Office of Science, U.S. Department of Energy is gratefully acknowledged. M.R. gratefully acknowledges support from the Alexander-von-Humboldt Foundation through the Feodor-Lynen program. We wish to thank Prof. Sunney Xie for useful discussions.

APPENDIX A: THE COHERENT HETERODYNE SIGNAL

Starting with Eq. (15), the density matrix to the nth order is given:

$$\rho^{(n)} = H'_-\left(\sum_{i=1}^{n} t_i\right) G(t_{n-1})\cdots G(t_2)H'_-(t_1) \times G(t_1)H'_-(0)\rho^{(0)}. \tag{A1}$$

The coherent n-D signal is given by

$$S^{(n)}_{\rm coh}(t_n,\ldots,t_1) = \left(\frac{-i}{\hbar}\right)^n {\rm tr}[H'_L G(t_n)H'_-\cdots G(t_2) \times H'_- G(t_1)H'_-\rho_0]. \tag{A2}$$

Compared to Eq. (13), we see that we have only one $\tilde{V}_L$ operator, where we have in the incoherent case a $\tilde{V}_L$ and $\tilde{V}_R$ operator. Since each $\tilde{V}_-$ represents a commutator this constitutes 2^n possible pathways. This can be seen by recasting Eq. (A2) in Hilbert space:

$$S^{(n)}_{\rm coh}(t_n,\ldots,t_1) = \left(\frac{-i}{\hbar}\right)^3 {\rm tr}\{H'(t_1+t_2+\cdots+t_n)[H'(t_1+\cdots+t_{n-1}),\ldots,[H'(t_1+t_2)[H'(t_1),[\tilde{V}(0),\rho]]]]\}. \tag{A3}$$

The third-order coherent signal has the form

$$S_{\rm coh}(t_3,t_2,t_1) = \left(\frac{-i}{\hbar}\right)^3 {\rm tr}[H'_L G(t_3) H'_- G(t_2) H'_- G(t_1) V_- \rho_0], \tag{A4}$$

$$S_{\rm coh}(t_3,t_2,t_1) = \left(\frac{-i}{\hbar}\right)^3 {\rm tr}\{H'(t_1+t_2+t_3)[H'(t_1+t_2)[H'(t_1),[H'(0),\rho_0]]]\}. \tag{A5}$$

This is the analog to Eq. (52).

Again we focus on the signal with phase $\varphi_4 = \varphi_1 + \varphi_2 - \varphi_3$. Other signals can be collected similarly for our model. In the rotating-wave approximation this has the two contributions (Fig. 5)

$$S_{\rm coh}(t_3,t_2,t_1) = \left(\frac{-i}{\hbar}\right)^3 {\rm tr}[V_L G(t_3) V_L G(t_2) V_L^\dagger G(t_1) V_L^\dagger \rho_0] E_\phi - \left(\frac{-i}{\hbar}\right)^3 {\rm tr}[V_L G(t_3) V_R G_(t_2) V_L^\dagger G(t_1) V_L^\dagger \rho_0] E_\phi. \tag{A6}$$

These can be recast using ordinary (Hilbert space) correlation functions:

$$S_{\rm coh}(t_3,t_2,t_1) = \left(\frac{-i}{\hbar}\right)^3 {\rm tr}[V(t_1+t_2+t_3)V(t_1+t_2)V^\dagger(t_1)V^\dagger(0)\rho_0]E_\phi - \left(\frac{-i}{\hbar}\right)^3 {\rm tr}[V(t_1+t_2)V(t_1+t_2+t_3)V^\dagger(t_1)V^\dagger(0)\rho_0]E_\phi. \tag{A7}$$

Expanding Eq. (A6) in system states, using the coherent limit Eq. (49), and using the approach of [32] to include the finite field envelopes finally gives

$$\begin{aligned} S_{\rm coh}(t_3,t_2,t_1) = {} & \left(\frac{-i}{\hbar}\right)^3 \sum_{g,e_1,e_2,f} P_{0,g} V_{ge_2} V_{e_2 f} V_{fe_1} V_{e_1 g} E_1(\omega_{e_1 g}) E_2(\omega_{fe_1}) E_3^*(\omega_{e_2 f}) E_4^*(\omega_{ge_2}) \exp\big(-i\omega_{e_2 g} t_3 - \gamma_{e_2 g} t_3 - i\omega_{fg} t_2 \\ & - \gamma_{fg} t_2 - i\omega_{e_1 g} t_1 - \gamma_{e_1 g} t_1\big) - \left(\frac{-i}{\hbar}\right)^3 \sum_{g,e_1,e_2,f} P_{0,g} V_{ge_2} V_{e_2 f} V_{fe_1} V_{e_1 g} E_1(\omega_{e_1 g}) E_2(\omega_{fe_1}) E_3^*(\omega_{ge_2}) E_4^*(\omega_{e_2 f}) \\ & \times \exp\big(-i\omega_{fe_2} t_3 - \gamma_{fe_2} t_3 - i\omega_{fg} t_2 - \gamma_{fg} t_2 - i\omega_{e_1 g} t_1 - \gamma_{e_1 g} t_1\big). \end{aligned} \tag{A8}$$

APPENDIX B: THE FIELD GREEN'S FUNCTION

Unlike in the rest of the paper, all operators in this appendix are given in the Heisenberg picture. The electric field obeys the usual homogeneous wave equation derived from Maxwell equations:

$$\nabla\times\nabla\times \boldsymbol{E}(\boldsymbol{r},\omega) - \frac{\omega^2}{c^2}\boldsymbol{E}(\boldsymbol{r},\omega) = \omega^2 \frac{1}{\varepsilon_0 c^2}\boldsymbol{V}_H(\boldsymbol{r},\omega). \tag{B1}$$

Here V is the molecular dipole moment and ε_0 is the vacuum permittivity. Since Eq. (B1) is linear it applies also for a quantum field, where the electric field and V become operators [24,39]. If we restrict ourselves to the transverse part in far field, this equation simplifies to

$$\nabla^2 \mathbf{E}(\boldsymbol{r},\omega) + \frac{\omega^2}{c^2}\mathbf{E}(\boldsymbol{r},\omega) = -\omega^2 \frac{1}{\varepsilon_0 c^2}\mathbf{V}_H(\boldsymbol{r},\omega). \tag{B2}$$

This equation can be solved using a Green function. For simplicity, we assume the Green function for an infinite space and ignore the polarization.

The Green function solution of Eq. (B2) for a single-point dipole molecule at $\boldsymbol{r} = 0$ is [28,40]

$$E(\boldsymbol{r},\omega) = -\frac{1}{\varepsilon_0 c^2}\omega^2 \frac{e^{i(\omega/c)|\boldsymbol{r}|}}{4\pi|\boldsymbol{r}|} V_H(0,\omega). \tag{B3}$$

In the time domain, this gives

$$E(\boldsymbol{r},t) = \frac{1}{\varepsilon_0 c^2}\frac{1}{4\pi|\boldsymbol{r}|}\partial_t^2 V_H(0,t-|\boldsymbol{r}|/c). \tag{B4}$$

The electric field which enters the gate at position $\boldsymbol{r}_G$ is given by

$$E(\boldsymbol{r}_G,t) = A\ddot{V}_H(0,t-|\boldsymbol{r}_G|/c), \tag{B5}$$

$$A = \frac{1}{\varepsilon_0 c^2}\frac{1}{4\pi|\boldsymbol{r}_G|}. \tag{B6}$$

To simplify the expressions, we will omit in the following the time retardation, assuming that the time scale at the detector is adjusted accordingly. We now write $\ddot{V}_H(0,t-|\boldsymbol{r}_G|/c) = \partial_t^2 V_H(0,t-|\boldsymbol{r}_G|/c)$.

The detector geometry may affect the signal, depending if an angle is used with a lens or if it enters in parallel. These details will affect the prefactor A and are not considered here.

APPENDIX C: GATING SPECTROGRAM FOR FREQUENCY GATE FOLLOWED BY TEMPORAL GATE

When the frequency gate is applied first, the gating spectrogram can be calculated similar to Eq. (7) and has the form [13]

$$\begin{aligned} W(\omega_0,t_0;\omega',t_1) = {} & \frac{1}{2\pi}\int_{-\infty}^{\infty} dt'' \int_{-\infty}^{\infty} d\tau e^{i\omega'\tau} F_t^*(t'';t_0) \\ & \times F_s^*(t''-t_1-\tau,\omega_0) F_t(t'';t_0) \\ & \times F_s(t''-t_1;\omega_0). \end{aligned} \tag{C1}$$

For the signal Eq. (10) holds in this case as well but the gating spectrogram is now given by

$$W(\omega_0,t_0;\omega',t_1) = \frac{1}{2\pi}\int_{-\infty}^{\infty} dt'' |F_t(t'';t_0)|^2 W_s(t''-t_1,\omega';\omega_0) \tag{C2}$$

with

$$W_s(t,\omega';\omega_0) = \int_{-\infty}^{\infty} d\tau e^{i\omega'\tau} F_s^*(t-\tau,\omega_0) F_s(t;\omega_0). \tag{C3}$$

APPENDIX D: SUM OVER STATE EXPRESSION FOR THE FLUORESCENCE SIGNAL WITH PHASE $\phi = \varphi_1 + \varphi_2 - \varphi_3 - \varphi_4$

Below we expand Eqs. (58)–(63) in eigenstates using the model system of Fig. 1 in the coherent limit Eq. (49):

$$S_{\mathrm{iia}}(\omega',t_4,t_3,t_2,t_1) = \frac{|A|^2}{\hbar^4} \sum_{e_1,e_2,e_3,f,g_1,g_2} P_{0,g_1}\left(-i\omega_{g_2e_3}-\gamma_{g_2e_3}\right)^2\left[-i\omega_{e_2g_2}-\left(\gamma_{e_2e_3}-\gamma_{g_2e_3}\right)\right]^2 E_1\left(\omega_{e_1g_1}-\omega_1\right)E_2\left(\omega_{fe_1}-\omega_2\right)$$
$$\times E_3^*\left(\omega_{fe_2}-\omega_3\right)E_4^*\left(\omega_{e_3g_1}-\omega_4\right)V_{g_1e_3}V_{e_3g_2}V_{g_2e_2}V_{e_2f}V_{fe_1}V_{e_1g_1}\frac{i}{-\left(\omega'+\omega_{g_2e_3}\right)+i\gamma_{g_2e_3}}$$
$$\times \exp\left(-i\omega_{e_2e_3}t_4-\gamma_{e_2e_3}t_4\right)\exp\left(-i\omega_{e_2g_1}t_3-\gamma_{e_2g_1}t_3-i\omega_{fg_1}t_2-\gamma_{fg_1}t_2-i\omega_{e_1g_1}t_1-\gamma_{e_1g_1}t_1\right), \tag{D1}$$

$$S^*_{\mathrm{iib}}(\omega',t_4,t_3,t_2,t_1) = \frac{|A|^2}{\hbar^4} \sum_{e_1,e_2,e_3,f,g_1,g_2} P_{0,g_1}\left(-i\omega_{e_2g_2}-\gamma_{e_2g_2}\right)^2\left[-i\omega_{g_2e_3}-\left(\gamma_{e_2e_3}-\gamma_{e_2g_2}\right)\right]^2 E_1\left(\omega_{e_1g_1}-\omega_1\right)E_2\left(\omega_{fe_1}-\omega_2\right)$$
$$\times E_3^*\left(\omega_{fe_2}-\omega_3\right)E_4^*\left(\omega_{e_3g_1}-\omega_4\right)V_{g_1e_3}V_{e_3g_2}V_{g_2e_2}V_{e_2f}V_{fe_1}V_{e_1g_1}\frac{-i}{\left(-\omega'+\omega_{e_2g_2}\right)-i\gamma_{e_2g_2}}$$
$$\times \exp\left(-i\omega_{e_2e_3}t_4-\gamma_{e_2e_3}t_4\right)\exp\left(-i\omega_{e_2g_1}t_3-\gamma_{e_2g_1}t_3-i\omega_{fg_1}t_2-\gamma_{fg_1}t_2-i\omega_{e_1g_1}t_1-\gamma_{e_1g_1}t_1\right), \tag{D2}$$

$$S_{\mathrm{iiia}}(\omega',t_4,t_3,t_2,t_1) = \frac{|A|^2}{\hbar^4} \sum_{e_1,e_2,e_3,f,g_1,g_2} P_{0,g_1}\left(-i\omega_{g_2e_3}-\gamma_{g_2e_3}\right)^2\left[-i\omega_{e_2g_2}-\left(\gamma_{e_2e_3}-\gamma_{g_2e_3}\right)\right]^2 E_1\left(\omega_{e_1g_1}-\omega_1\right)E_2\left(\omega_{fe_1}-\omega_2\right)$$
$$\times E_3^*\left(\omega_{e_3g_1}-\omega_3\right)E_4^*\left(\omega_{fe_2}-\omega_4\right)V_{g_1e_3}V_{e_3g_2}V_{g_2e_2}V_{e_2f}V_{fe_1}V_{e_1g_1}\frac{i}{-\left(\omega'+\omega_{g_2e_3}\right)+i\gamma_{g_2e_3}}$$
$$\times \exp\left(-i\omega_{e_2e_3}t_4-\gamma_{e_2e_3}t_4\right)\exp\left(-i\omega_{fe_3}t_3-\gamma_{fe_3}t_3-i\omega_{fg_1}t_2-\gamma_{fg_1}t_2-i\omega_{e_1g_1}t_1-\gamma_{e_1g_1}t_1\right), \tag{D3}$$

$$S^*_{\mathrm{iiib}}(\omega',t_4,t_3,t_2,t_1) = \frac{|A|^2}{\hbar^4} \sum_{e_1,e_2,e_3,f,g_1,g_2} P_{0,g_1}\left(-i\omega_{e_2g_2}-\gamma_{e_2g_2}\right)^2\left[-i\omega_{g_2e_3}-\left(\gamma_{e_2e_3}-\gamma_{e_2g_2}\right)\right]^2 E_1\left(\omega_{e_1g_1}-\omega_1\right)E_2\left(\omega_{fe_1}-\omega_2\right)$$
$$\times E_3^*\left(\omega_{e_3g_1}-\omega_3\right)E_4^*\left(\omega_{fe_2}-\omega_4\right)V_{g_1e_3}V_{e_3g_2}V_{g_2e_2}V_{e_2f}V_{fe_1}V_{e_1g_1}\frac{-i}{\left(-\omega'+\omega_{e_2g_2}\right)-i\gamma_{e_2g_2}}$$
$$\times \exp\left(-i\omega_{e_2e_3}t_4-\gamma_{e_2e_3}t_4\right)\exp\left(-i\omega_{fe_3}t_3-\gamma_{fe_3}t_3-i\omega_{fg_1}t_2-\gamma_{fg_1}t_2-i\omega_{e_1g_1}t_1-\gamma_{e_1g_1}t_1\right), \tag{D4}$$

$$S_{\mathrm{iva}}(\omega',t_4,t_3,t_2,t_1) = -\frac{|A|^2}{\hbar^4} \sum_{e_1,e_2,e_3,f_1,f_2,g_1} P_{0,g_1}\left(-i\omega_{e_3f_2}-\gamma_{e_3f_2}\right)^2\left[-i\omega_{f_1e_3}-\left(\gamma_{f_1f_2}-\gamma_{e_3f_2}\right)\right]^2 E_1\left(\omega_{e_1g_1}-\omega_1\right)E_2\left(\omega_{f_1e_1}-\omega_2\right)$$
$$\times E_3^*\left(\omega_{e_2g_1}-\omega_3\right)E_4^*\left(\omega_{f_2e_2}-\omega_4\right)V_{g_1e_2}V_{e_2f_2}V_{f_2e_3}V_{e_3f_1}V_{f_1e_1}V_{e_1g_1}\frac{i}{-\left(\omega'+\omega_{e_3f_2}\right)+i\gamma_{e_3f_2}}$$
$$\times \exp\left(-i\omega_{f_1f_2}t_4-\gamma_{f_1f_2}t_4\right)\exp\left(-i\omega_{f_1e_2}t_3-\gamma_{f_1e_2}t_3-i\omega_{f_1g_1}t_2-\gamma_{f_1g_1}t_2-i\omega_{e_1g_1}t_1-\gamma_{e_1g_1}t_1\right), \tag{D5}$$

$$S^*_{\mathrm{ivb}}(\omega',t_4,t_3,t_2,t_1) = -\frac{|A|^2}{\hbar^4} \sum_{e_1,e_2,e_3,f_1,f_2,g_1} P_{0,g_1}\left(-i\omega_{f_1e_3}-\gamma_{f_1e_3}\right)^2\left[-i\omega_{e_3f_2}-\left(\gamma_{f_1f_2}-\gamma_{f_1e_3}\right)\right]^2 E_1\left(\omega_{e_1g_1}-\omega_1\right)E_2\left(\omega_{f_1e_1}-\omega_2\right)$$
$$\times E_3^*\left(\omega_{e_2g_1}-\omega_3\right)E_4^*\left(\omega_{f_2e_2}-\omega_4\right)V_{g_1e_2}V_{e_2f_2}V_{f_2e_3}V_{e_3f_1}V_{f_1e_1}V_{e_1g_1}\frac{-i}{\left(-\omega'+\omega_{f_1e_3}\right)-i\gamma_{f_1e_3}}$$
$$\times \exp\left(-i\omega_{f_1f_2}t_4-\gamma_{f_1f_2}t_4\right)\exp\left(-i\omega_{f_1e_2}t_3-\gamma_{f_1e_2}t_3-i\omega_{f_1g_1}t_2-\gamma_{f_1g_1}t_2-i\omega_{e_1g_1}t_1-\gamma_{e_1g_1}t_1\right). \tag{D6}$$

[1] S. Mukamel, *Principles of Nonlinear Optical Spectroscopy* (Oxford University Press, New York, 1995).
[2] A. M. Weiner, *Ultrafast Optics* (Wiley, New York, 2009).
[3] P. Corkum, S. D. Silvestri, K. A. Nelson, E. Riedle, and R. W. Schoenlein, *Ultrafast Phenomena XVI* (Springer, 2009).
[4] E. Barkai, F. Brown, M. Orrit, and H. Yang, *Modeling and Evaluation of Single Molecule Measurements* (World Scientific, Singapore, 2008).
[5] W. E. Moerner and D. P. Fromm, Rev. Sci. Instrum. **74**, 3597 (2003).
[6] J. Elf, G.-W. Li, and X. S. Xie, Science **316**, 1191 (2007).
[7] R. R. Ernst, G. Bodenhausen, and A. Wokaun, *Principles of Nuclear Magnetic Resonance in One or Two Dimensions* (Clarendon, Oxford, 1998).
[8] C. Scheurer and S. Mukamel, J. Chem. Phys. **115**, 4989 (2001).
[9] C. Scheurer and S. Mukamel, Bull. Chem. Soc. Jpn. **75**, 989 (2002).
[10] P. Tian, D. Keusters, Y. Suzaki, and W. S. Warren, Science **300**, 1553 (2003).
[11] J. H. Eberly and K. Wódkiewicz, J. Opt. Soc. Am. **67**, 1252 (1977).
[12] H. Stolz, *Time-Resolved Light Scattering from Excitons*, Vol. 130 of Springer Tracts in Modern Physics (Springer-Verlag, Berlin, 1994).
[13] S. Mukamel, C. Ciordas-Ciurdariu, and V. Khidekel, IEEE J. Quantum Electron. **32**, 1278 (1996).
[14] S. Mukamel, C. Ciordas-Ciurdariu, and V. Khidekel, Adv. Chem. Phys. **101**, 345 (1997).
[15] S. Mukamel, J. Chem. Phys. **107**, 4165 (1997).
[16] M. Cho, N. F. Scherer, G. R. Fleming, and S. Mukamel, J. Chem. Phys. **96**, 5618 (1992).
[17] T. J. Dunn, I. A. Walmsley, and S. Mukamel, Phys. Rev. Lett. **74**, 884 (1995).
[18] P. F. Tekavec, T. R. Dyke, and A. H. Marcus, J. Chem. Phys. **125**, 194303 (2006).
[19] P. F. Tekavec, G. A. Lott, and A. H. Marcus, J. Chem. Phys. **127**, 214307 (2007).
[20] J. A. Cina, Annu. Rev. Phys. Chem. **59**, 319 (2008).
[21] G. A. Lott, A. Perdomo-Ortiz, J. K. Utterback, A. Aspuru-Guzik, and A. H. Marcus*, PNAS (unpublished, submitted) (2010).
[22] D. Brinks, F. D. Stefani, F. Kulzer, R. Hildner, T. H. Taminiau, Y. Avlasevich, K. Müllen, and N. F. van Hulst, Nature **465**, 905 (2010).
[23] S. Weiss, Science **283**, 1676 (1999).
[24] C. Cohen-Tannoudji and A. G. G. Jacques Dupont-Roc, *Atom-Photon Interactions* (Wiley, New York, 1992).
[25] M. O. Scully and M. S. Zubairy, *Quantum Optics* (Cambridge University Press, Cambridge, 1997).
[26] B. R. Mollow, Phys. Rev. A **2**, 76 (1970).
[27] R. J. Glauber, *Quantum Theory of Optical Coherence* (Wiley-VCH, 2007).
[28] R. P. Feynman, R. B. Leighton, and M. Sands, *The Feynman Lectures on Physics I* (Addison-Wesley, New York, 1963), chap. 30, pp. 10–12.
[29] A. E. Cohen and S. Mukamel, Phys. Rev. Lett. **91**, 233202 (2003).
[30] U. Harbola and S. Mukamel, Phys. Rep. **465**, 191 (2008).
[31] O. Roslyak and S. Mukamel, *Spontaneous and Stimulated Coherent and Incoherent Nonlinear Wave-Mixing and Hyper-Raleigh Scattering* (Lectures of Virtual European University, Max-Born Institute, EVU Lecture Notes, 2010), [http://www.mitr.p.lodz.pl/evu/lectures/mukamel.pdf].
[32] I. V. Schweigert and S. Mukamel, Phys. Rev. A **77**, 03380212 (2008).
[33] F. Šanda, V. Perlík, and S. Mukamel, J. Chem. Phys. **133**, 014102 (2010).
[34] O. Roslyak and S. Mukamel, Mol. Phys. **107**, 265 (2009).
[35] U. Höfer, I. L. Shumay, C. Reuß, U. Thomann, W. Wallauer, and T. Fauster, Science **277**, 1480 (1997).
[36] T. Klamroth, P. Saalfrank, and U. Höfer, Phys. Rev. B **64**, 035420 (2001).
[37] M. Aeschliemann, T. Brixner, A. Fischer, C. Kramer, P. Melchior, W. Pfeiffer, C. Schneider, C. Strüber, P. Tuchscherer, and D. V. Voronine, coherent two-dimensional nanoscopy. (unpublished, submitted to science).
[38] S. Rahav and S. Mukamel, Phys. Rev. A **81**, 063810 (2010).
[39] S. Rahav and S. Mukamel, J. Chem. Phys. **133**, 244106 (2010).
[40] W. Vogel and D.-G. Welsch, *Quantum Optics*, 3rd ed. (Wiley-VCH, Weinheim, 2006).